Fragility curves for low-damage rocking dissipative connections of precast concrete buildings

Michele Matteoni[1], Jonathan Ciurlanti[2], Simona Bianchi[3] and Stefano Pampanin[1]

[1]*Department of Structural and Geotechnical Engineering,*
Sapienza University of Rome,
Via Eudossiana 18, 00184 Rome, Italy

[2]*Arup Netherlands,*
Naritaweg 118, 1043 CA Amsterdam, The Netherlands

[3]*Department of Architectural Engineering,*
Delft University of Technology,
Mekelweg 5, 2628 CD Delft, The Netherlands

Abstract
Different low-damage technologies have recently been developed to meet society's growing expectations for earthquake-proof buildings. Among others, the PRESSS (PREcast Seismic Structural System) technology has proved its capability to withstand earthquakes with minimal damage, effectively mitigating socio-economic losses. However, applying loss assessment methodologies can pose challenges due to the lack of data regarding fragility functions for low-damage structural components. This paper aims to propose a method for computing numerical fragility curves for rocking dissipative structural components. To achieve this, archetypes of precast concrete structures were analyzed to develop fragility models for this technology.

1 Introduction

Recent catastrophic seismic events have further highlighted the urgent need for building a safer urban environment and enhancing community resilience. Following the Canterbury earthquake sequence in 2010-2011, society abruptly realised that even up-to-date code-compliant buildings were prone to extensive damage, often leading to non-economically viable repairs [1]. This mismatch between the public's expectations and what the common engineering practice provided, shined a light on newly developed low-damage (or damage-control) solutions.

Among others, the so-called PRESSS technology (PREcast Seismic Structural System, [2]-[5]), originally developed at University of California San Diego at the end of the last century and further refined and extensively tested at University of Canterbury in New Zealand with several implementations on-site around the world, proved to be an effective solution in mitigating seismic damage ([1], [5]-[8]). This technology employs a combination of unbonded post-tensioning systems, providing recentring capabilities thus minimizing residual deformations, along with mild steel elements, offering additional damping to the structure (Figure 1). The precast elements can accommodate large relative displacements without incurring damage, thanks to a controlled rocking mechanism. The dry-jointed ductile connections between precast elements develop a controlled rocking mechanism at the interface where the deformation is concentrated through the opening and closing of a gap. Mild steel elements can be located externally to the section by encasing them in replaceable "Plug&Play" dissipation devices, further reducing downtime and repair costs [9].

The success of such technology has led to several on-site applications, employing different materials as well, such as steel [10] and timber (referred to as Pres-Lam technology, [11]).

Recent numerical and experimental studies, supported by evidences from the actual response under earthquake events, have shown that this technology not only provides an outstanding seismic performance but also effectively reduces direct and indirect economic losses, especially when combined with low-damage non-structural systems [12].

Despite the growing interest in such technology, assessing the seismic performance of low-damage structures using a component-based loss assessment methodology, such as FEMA P-58 [13] can be challenging due to the lack of information regarding fragility functions for rocking-dissipative structural components. Previous works proposed models for fragility curves based on experimental results (e.g. [14]). However, such results were based on a limited amount of data, constrained by the relative novelty of the technology and the relatively low quantity of experimental testing available when compared to traditional systems.

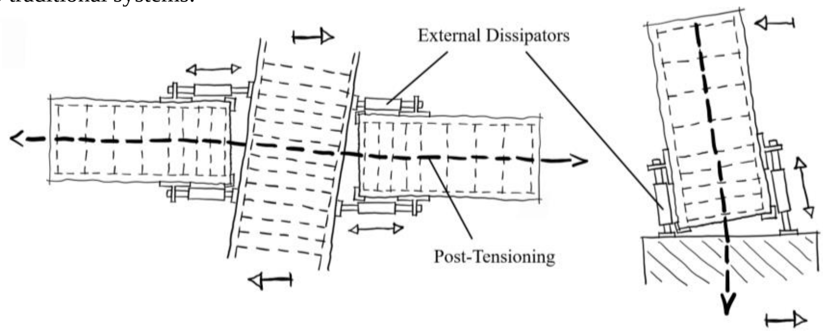

Fig. 1 Overview of the PRESSS structural connections with external Plug&Play dissipators: beam-column subassembly (left) column-foundation interface (right).

To this end, this paper aims to develop and propose numerical-based fragility curves for structural components of PRESSS frame systems, accounting for record-to-record variability and material uncertainties. To accomplish this task, the Bayesian CLOUD methodology [15] was employed by performing several Non-Linear Time History Analyses (NLTHAs) on different case studies, modelled using the open-source software OpenSEES [16].

2 Methodology

To compute fragility curves, the Bayesian CLOUD analysis ([17], [15]) was implemented due to its ability to consider multiple sources of uncertainties. The methodology employs a suite of unscaled ground motions pairing them with multiple realizations/configurations of the structure generated by employing a standard Monte Carlo simulation. The output data can be subsequently used to fit fragility functions.

Component fragility functions can be developed by applying the CLOUD methodology to model the correlation between an Engineering Demand Parameter (EDP) parameter and a structural component's Demand Capacity Ratio (DCR). In this study, the chosen EDP is the inter-storey drift ratio for consistency with the FEMA P-58 methodology. The DCR is calculated separately for every structural connection of the building. The limit state (or damage) thresholds are determined specifically for each structural connection. The computed limit state thresholds are then compared to the maximum gap openings that occur during the Non-Linear Time History Analyses (NLTHAs).

It is worth highlighting that the CLOUD methodology is particularly well-suited for this numerical application because it dispenses with scaling the ground motions entirely, avoiding the recursive scaling processes typical of other methodologies, such as Incremental Dynamic Analyses (IDA, [18]).

Finally, for further comparison, fragility functions were also derived without considering the material uncertainties (i.e. considering the median values for the materials).

2.1 Determination of the fragility functions

To fit the fragility models, a simple linear regression in the logarithmic space was employed, without taking into account collapse cases and failed analyses. Therefore, cases that experienced a maximum inter-storey drift ratio of more than 10% or failed due to dynamic instability were excluded from the dataset. Furthermore, analyses that exhibited a maximum inter-storey drift of less than 0.05% were also excluded from the dataset, as the ground motions were not strong enough to engage the structural connections.

Fragility functions can be expressed as a logNormal Cumulative Distribution Function (CDF) :

$$P[DCR_{LS} > 1|EDP] = CDF\left(\frac{E[lnDCR_{LS}|EDP]}{\beta_{DCR_{LS}}}\right) \tag{1}$$

Where $P[DCR_{LS} > 1|EDP, NoC]$ is the probability of exceeding a defined limit state given an EDP, $E[lnDCR_{LS}|EDP]$ is the expected value of $lnDCR$ given an EDP, and $\beta_{DCR_{LS}}$ is the logNormal standard deviation. The expected value can be fitted using linear regression in the log-log space:

$$E[lnDCR_{LS}|EDP] = lna + b \cdot ln(EDP) \tag{2}$$

Where $lna\ and\ b$ are the fitting parameters.

Finally, the dispersion can be assessed by computing the logarithmic standard deviation:

$$\beta_{DCR_{LS}} \simeq \sigma_{lnDCR_{LS}} = \sqrt{\sum_{i}^{n}\left(lnDCR_{LS,i} - E[lnDCR_{LS}|EDP_i]\right)^2 / (N-2)} \tag{3}$$

2.2 Determination of the fragility functions

To consider the uncertainties related to the materials, the properties of the mild steel and the concrete were assumed to follow a logNormal distribution. The tendons' properties were instead considered as deterministic values because the variability related to tendons' proprieties is out weighted by other sources of uncertainty. Furthermore, the tendons are designed to remain elastic until the offset of the investigated limit state. As a result The Latin Hypercube Sampling (LHS) methodology [19] was used to produce the different realizations of uncertain material properties to be randomly paired with an earthquake record from the selected pool. The parameters adopted for the probabilistic distributions of the material properties are shown in Table 1.

Table 1 Parameters of the probabilistic distributions.

Parameter	Symbol	Unit	Mean	COV	Reference
Steel reinforcement yield stress	f_{yk}	[MPa]	450	0.05	[20]
Steel reinforcement Young modulus	E_s	[GPa]	210	0.05	[21]
Steel reinforcement ultimate strain	ε_{su}	[%]	6	0.15	[22]
Concrete compressive strength	f_{ck}	[MPa]	50	0.20	[20]
Concrete strain at peak stress	ε_{cc}	[%]	0.21	0.10	[22]
Confined concrete ultimate strain	ε_{cu}	[%]	1	0.20	[22]

3 Case Studies

The analyses were performed on three different multi-storey reinforced concrete buildings characterized by the same plan of 32 m x 18 m, and different total height (3, 5, and 7 storeys, respectively). The building scheme derives from a previous study developed by [12].

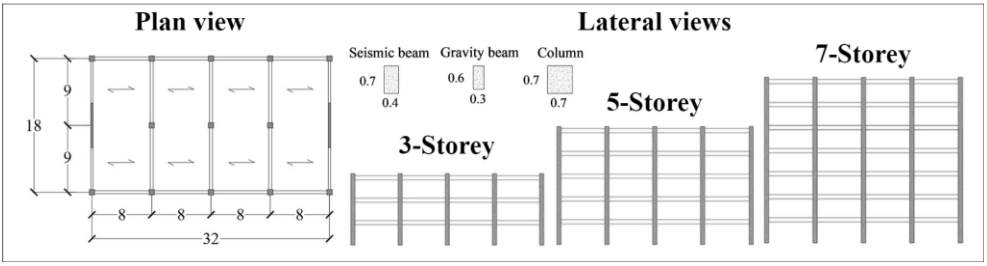

Fig. 2 Overview of the structural systems of the case-study buildings.

The lateral resisting systems of the building are composed of two four-bay frames along the longitudinal direction and two shear walls along the transverse direction. All the case studies have an interstorey height of 3.8m and the building use is commercial. This paper focuses on the behaviour of the frame direction only, as its main purpose is to develop fragility function for the frames' structural sub-assemblies. An overview of the case studies geometry is presented in Figure 2. The buildings were designed considering vertical loads (self-weight and live loads) and horizontal loads of a high seismic area in Sourthern Italy (Reggio Calabria, soil type C). The structures were designed following the Direct Displacement-Based Design (DDBD, [23]). Additional information regarding the structural design can be found in [12]. All the case study buildings employ low-damage PRESSS hybrid connections.

3.1 Modelling approach

A parametric 2D model was implemented in OpenSEES [16] by using the Python API [24]. The structural skeleton was modelled following a lumped plasticity approach as proposed by [25]. The structural framing was modelled by means of elastic frame elements and rigid joint panels. To consider the non-linear behaviour of the hybrid connections, two parallel rotational springs were defined at each end of the beams and the base column's interfaces. The two rotational springs were defined using: i) an ElasticMultiLinear element to model the re-centring behaviour of the unbonded tendon, and ii) a Giuffrè-Meegotto-Pinto (GMP) link to model the plastic behaviour of the external dissipators. The parameters of the links were defined from the section analysis performed on each connection for each realization of the building. The friction between tendons and the ducts is not considered in the model.

In the section analysis, the behaviour of the external damping devices was modelled using an elasto-plastic rule with hardening, and the confined concrete was modelled using the [26] constitutive model assuming a confinement ratio of 1.25. The unbonded tendon was modelled as linear elastic as the section is considered to have failed beyond the tendon's yielding. To model the failure of the sections, both links were wrapped into a MinMax material, available in the OpenSEES library. Soil-structure interaction was neglected.

3.2 Definition of damage states

Two different damage conditions (limit states) were considered for the low-damage PRESSS structural connections, as in [12]: i) the failure of the external dissipators, defined as the overcoming of the ultimate strain value (DS1), and ii) the yielding of the unbonded tendons/bars (DS2). These limit states were expressed as the gap opening corresponding to each damage level as computed during the section analysis phase for each beam/column section.

4 Record Selection

A total of 141 ground motions were chosen from the NGA PEER West2 Database [27] the same adopted by [28]. The selected ground motions' spectra, as well as the intensity measures, chosen as the first-period spectral acceleration, for all three different case studies, are shown in Figure 3.

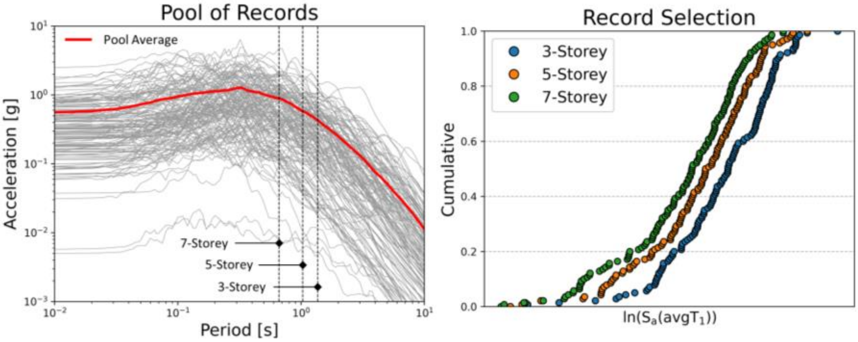

Fig. 3 Spectra of the selected pool of records for the CLOUD analysis (left), and distribution of the intensity measures - $S_a(avg(T_1))$ - for each case study (right). Graphs always refer to the average first natural period T_1 of the different realizations of each case study.

Due to the high seismic performance of low-damage structural systems, the desired ratio of 30% of failure cases, as recommended by [15], could not be achieved using unscaled ground motions for the DS2 limit state. Despite that, the decision was made to continue with the current suite of records without recurring to a scaling procedure.

5 Results and Discussion

For each case study, 141 realizations were sampled and each sample was then paired with one of the ground motions: 423 NLTHAs were performed. A total of 30 distinct beam-column connections (15 internal and 15 external) and 6 column-foundation connections (3 internal and 3 external) were analyzed. After removing cases which led to a max drift of over 10%, failed cases and cases which did not overcome an inter-storey drift of 0.05%, 4016 unique datapoints for beam-column connections and 798 for column-foundation connections were left in the dataset.

The various connections were characterised by different reinforcement details, post-tensioning specifications and location in the case-study buildings, thus leading to an increased variability. The datasets and the regressions in the logarithmic plane are presented in Figure 4.

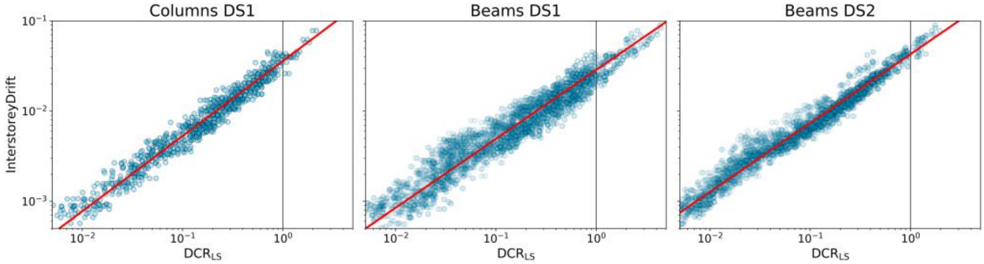

Fig. 4 Cloud models for component type and damage states: mild steel rupture in column-foundation connections (left), mild steel rupture in beam-column connections (centre), and tendon yielding in beam-column connections (right).

Data is well fitted by a simple linear regression in the logarithmic plane for all the cases. Results show a dispersion (beta) in the range of 0.27-0.41, with the maximum value obtained for DS1 of column connections (as shown in Table 2). Although the tendon was considered deterministic, DS2 for beams shows a dispersion of 0.27 due to the variability in section details and concrete uncertainties. On the other hand, columns show a similar value of beta due to the reduced number of available datapoints and connection types. Column-foundation connections are indeed characterized by similar reinforcement details and are always located on the ground floor.

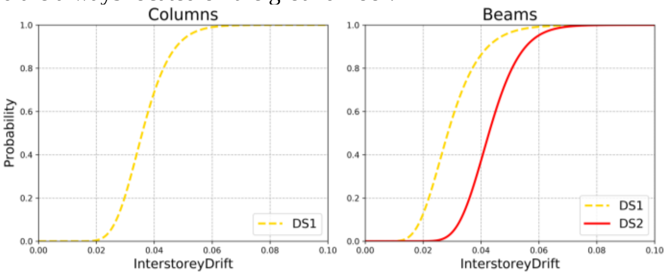

Fig. 5 Fragility curves for column-foundation connections (left) and beam-column connections (right).

Finally, it is worth noting how the dispersion in the logarithmic plane, in the case of beam-column connections, tends to decrease while the DCR increases. This happens because, for lower values of inter-storey drift and DCR, the dataset tends to deviate from the linear regression.

Table 2 Parameters of the fragility curves for both beams and columns.

Connection	Damage State	Unit	Mean	Beta
Column	DS1	[%]	3.58	0.267
Beam	DS1	[%]	2.85	0.406
Beam	DS2	[%]	4.27	0.266

It is found that the median value of the fragility curves related to damage state DS1 for beam-column connections, about 2.9%, is less than the one related to the same level of damage but in the column-foundation connections, around 3.6%. This is caused by the size of the external damping devices, characterized by a larger diameter at the base column's sections, leading to longer dissipators' fuses (maintaining slenderness constant) and thus reducing strain values for the same rotations. This was expected because the inter-storey drift of the ground floor is usually considered as the critical drift in the displacement-based design approach for frame systems, leading to a more cautionary design for column-foundation connections. Computed fragility curves are represented in Figure 5.

5.1 Impact of material uncertainties

To quantify the effect that material uncertainties have on the above-discussed results, analyses were repeated considering the median values for the material properties. Following the same approach, the number of valid datapoints increased to 804 and 4044 for column-foundation and beam-column connections, respectively. Regression curves are presented in Figure 6.

Results show that the median values remain the same, exception made of a slight difference concerning the DS2 limit state, while the dispersion decreases. The beta/dispersion value related to material uncertainty was quantified from the decrease in dispersion. Specifically, by removing the beta value due to record-to-record and section-to-section variability (β_(REC-SEC)) from the beta accounting for all the uncertainties (β_TOT). The value of beta from the material uncertainty (β_MAT) can be assessed by means of the following expression:

$$\beta_{MAT} = \sqrt{\beta_{TOT}^2 - \beta_{REC-SEC}^2} \tag{4}$$

It is finally found that material uncertainties account for an additional beta value of around 0.16 slightly higher for DS1 limit states while slightly lower for DS2 limit states, as expected.

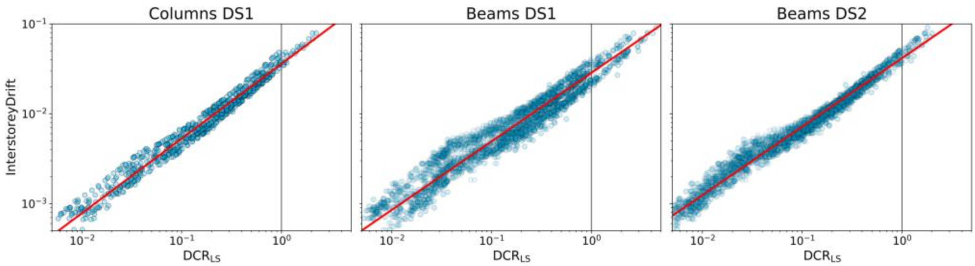

Fig. 6 Cloud models for component type and damage states not accounting for material uncertainties: mild steel rupture in column-foundation connections (left), mild steel rupture in beam-column connections (centre), and tendon yielding in beam-column connections (right).

Table 3 Parameters of the fragility curves and beta values for both beams and columns related to material uncertainty alone.

Connection	Damage State	Unit	Mean	Beta	Beta (MAT)
Column	DS1	[%]	3.58	0.217	0.156
Beam	DS1	[%]	2.85	0.369	0.169
Beam	DS2	[%]	4.15	0.222	0.147

6 Conclusions

This paper has developed and proposed models for the fragility functions of low-damage structural connections for PRESSS technology. The Bayesian CLOUD Methodology was implemented to fit a relationship between the Demand Capacity Ratio (DCRs) of the various components with the relative inter-storey drift, chosen as the Engineering Demand Parameter (EDP). The investigated damage states were the rupture of the external mild steel damping devices (DS1) and the yielding of the post-tensioned unbonded tendons (DS2). A parametric study was developed to perform several Non-Linear Time

History Analyses (NLTHAs) for three different case studies characterized by different structural sections and number of storeys, as well as different material proprieties.

The results showed that the first damage state (DS1) for beam-column connections is expected to occur around an inter-storey drift value of around 2.9% while the same damage state for column-foundation connections is expected to occur for values around 3.6%. Furthermore, results showed that, although beam-column connections are expected to be damaged at a lower drift value, they were affected by higher variability, showing a dispersion value of around 0.41. Finally, the more severe damage state (DS2) was found to occur at drift values around 4.3% with a relatively low dispersion of 0.27, when compared to the DS1 damage state. This was due to the reduced variability in terms of both material uncertainty and reinforcement variability, as the mild steel does not contribute after the DS1 damage state is overcome. Furthermore, material uncertainties provided a dispersion of around 0.16, with lower values for the DS2 of beam-column connections, thereby affecting to a lesser extent the results than section-to-section and record-to-record variability.

Data regarding the concrete core crushing was not presented in this paper, as the data obtained from the implemented analyses was deemed inconclusive and further investigation is needed to make any meaningful remark. Moreover, to better assess the dispersion of the column-foundation connections, a wider variety of case studies should be evaluated. Additionally, the reliability of the results could be increased by introducing the model uncertainties and by employing a robust-fragility methodology. Finally, consequence functions (repair time and cost) should be defined for the investigated damage states, to provide complete fragility specifications of this technology thus enabling loss assessment analysis.

Acknowledgements

The first author's PhD scholarship has been provided by the PNRR funding scheme (Piano Nazionale di Ripresa e Resilienza, in Italian) as part of the National Research Centre CN1 on "High-Performance Computing, Big Data and Quantum Computing" - Spoke 5Environment & Natural Disaster: Framework and methodologies for impact evaluation and risk mitigation, whose support is greatly appreciated.

References

[1] Pampanin, Stefano. 2012. “Reality-Check and Renewed Challenges in Earthquake Engineering.” *Bulletin of the New Zealand Society for Earthquake Engineering* 45(4):137–60. doi:10.5459/bnzsee.45.4.137-160.

[2] Priestley, M. J. Nigel. 1991. “Overview of PRESSS Research Program.” *PCI Journal* 36(4):50–57. doi:10.15554/pcij.07011991.50.57.

[3] Stanton, John, William C. Stone, and Geraldine S. Cheok. 1997. “A Hybrid Reinforced Precast Frame for Seismic Regions.” *PCI Journal* 42(2):20–23. doi:10.15554/pcij.03011997.20.23.

[4] Priestley, M. J. Nigel, S. (Sri) Sritharan, James R. Conley, and Stefano Stefano Pampanin. 1999. “Preliminary Results and Conclusions from the PRESSS Five-Story Precast Concrete Test Building.” *PCI Journal* 44(6):42–67. doi:10.15554/pcij.11011999.42.67.

[5] Pampanin, Stefano. 2005. “Emerging Solutions for High Seismic Performance of Precast/Prestressed Concrete Buildings.” *Journal of Advanced Concrete Technology* 3(2):207–23.

[6] Pampanin, Stefano, Dion Marriott, and Alessandro Palermo. 2010. *PRESSS design handbook* . New Zealand Concrete Society.

[7] Pampanin, Stefano. 2022. "NextGen building systems - S4: Seismically safer, sustainable and smart - raising the bar to enhance community resilience and sustainability." *In Springer Proceedings in Earth and Environmental Sciences*:343–362. doi:10.1007/978-3-031-15104-0_21.

[8] Pampanin, Stefano, Jonathan Ciurlanti, Simona Bianchi, Daniele Perrone, Gabriele Granello, Michele Palmieri, Damian N. Grant, et al. 2023. "Triaxial shake table testing of an integrated low-damage building system." *Earthquake Engineering & Structural Dynamics*, *52*(10), 2983–3007. doi:10.1002/eqe.3906.

[9] Sarti, Francesco, Alessando Palermo, and Stefano Pampanin. 2016. “Fuse-Type External Replaceable Dissipators: Experimental Program and Numerical Modeling.” *Journal of Structural Engineering* 142(12). doi:10.1061/(asce)st.1943-541x.0001606.

[10] Christopoulos, Constantin, Andre Filiatrault, Chia-Ming Uang, and Bryan Folz. 2002. “Post-tensioned Energy Dissipating Connections for Moment-Resisting Steel Frames.” *Journal of Structural Engineering* 128(9):1111–20. doi:10.1061/(asce)0733-9445(2002)128:9(1111).

[11] Palermo, Alessandro, Stefano Pampanin, Andy Buchanan, and Michael P. Newcombe. 2005. "Seismic design of multi-storey buildings using laminated veneer lumber (LVL)." Paper presented at New Zealand Society for Earthquake Engineering Conference, Wairakei, Taupo, New Zealand.

[12] Bianchi, Simona, Jonathan Ciurlanti, and Stefano Pampanin. 2021. "Comparison of Traditional vs Low-Damage Structural and Non-Structural Building Systems through a Cost/Performance-Based Evaluation." *Earthquake Spectra: The Professional Journal of the Earthquake Engineering Research Institute* 37(1):366–85. doi:10.1177/8755293020952445.

[13] Federal Emergency Management Agency (FEMA). 2012. *Seismic performance assessment of buildings, volume 1—Methodology*. Technical report FEMA P-58-1, Washington, DC.

[14] Nuzzo, Iolanda, Stefano Pampanin, and Nicola Caterino. 2018. "Proposal of a new loss ratio performance matrix in seismic design framework." Paper presented at the 16th European conference on earthquake engineering, Thessaloniki, Greece, June, 18–21.

[15] Jalayer, Fatemeh, Raffaele De Risi, and Gaetano Manfredi. 2015. "Bayesian Cloud Analysis: Efficient Structural Fragility Assessment Using Linear Regression." *Bulletin of Earthquake Engineering* 13(4):1183–1203. doi:10.1007/s10518-014-9692-z.

[16] McKenna, Frank. 2011. "OpenSees: A Framework for Earthquake Engineering Simulation." *Computing in Science & Engineering* 13(4):58–66. doi:10.1109/mcse.2011.66.

[17] Jalayer, Fatemeh, Ludovica Elefante, Iunio Iervolino, and Gaetano Manfredi. 2011. "Knowledge-Based Performance Assessment of Existing RC Buildings." *Journal of Earthquake Engineering* 15(3):362–89. doi:10.1080/13632469.2010.501193.

[18] Vamvatsikos, Dimitrios, and C. Allin Cornell. 2002. "Incremental Dynamic Analysis." *E-arthquake Engineering & Structural Dynamics* 31(3):491–514. doi:10.1002/eqe.141.

[19] Helton, Jon C., and F. J. Davis. 2003. "Latin hypercube sampling and the propagation of uncertainty in analyses of complex systems." *Reliability Engineering & System Safety*, *81*(1), 23–69. doi:10.1016/s0951-8320(03)00058-9

[20] Celarec, Daniel, and Matjaz Dolšek. 2013. "The Impact of Modelling Uncertainties on the Seismic Performance Assessment of Reinforced Concrete Frame Buildings." *Engineering Structures* 52:340–54. doi:10.1016/j.engstruct.2013.02.036.

[21] Hess, Paul E., Daniel Bruchman, Ibrahim A. Assakkaf, and Bilal M. Ayyub. 2002. "Uncertainties in Material and Geometric Strength and Load Variables." *Naval Engineers Journal* 114(2):139–66. doi:10.1111/j.1559-3584.2002.tb00128.x.

[22] Barbato, Michele, Quan Gu, and Joel P. Conte. 2010. "Probabilistic Push-over Analysis of Structural and Soil-Structure Systems." *Journal of Structural Engineering* 136(11):1330–41. doi:10.1061/(asce)st.1943-541x.0000231.

[23] Priestley, M. J. Nigel. 2002. "Direct Displacement-Based Design of Precast/Prestressed Concrete Buildings." *PCI Journal* 47(6):66–79. doi:10.15554/pcij.11012002.66.79.

[24] Zhu, Minjie, Frank McKenna, and Michael H. Scott. 2018. "OpenSeesPy: Python Library for the OpenSees Finite Element Framework." *SoftwareX* 7:6–11. doi:10.1016/j.softx.2017.10.009.

[25] Pampanin, Stefano, M. J. Nigel Priestley, and S. (Sri) Sritharan. 2001. "Analytical Modelling of the Seismic Behaviour of Precast Concrete Frames Designed with Ductile Connections." *Journal of Earthquake Engineering* 5(3):329–67. doi:10.1080/13632460109350397.

[26] Mander, John B., M. J. Nigel Priestley, and Robert Park. 1988. "Theoretical Stress-strain Model for Confined Concrete." *Journal of Structural Engineering* 114(8):1804–26.

[27] Ancheta, Timothy D., Robert B. Darragh, Jonathan P. Stewart, Emel Seyhan, Walter J. Silva, Brian S-J Chiou, Katie E. Wooddell, et al. 2014. "NGA-West2 Database." *Earthquake Spectra: The Professional Journal of the Earthquake Engineering Research Institute* 30(3):989–1005. doi:10.1193/070913eqs197m.

[28] Jalayer, Fatemeh, Hossein Ebrahimian, and Andrea Miano. 2021. "Record-to-record variability and code-compatible seismic safety-checking with limited number of records". *Bulletin of E-arthquake Engineering*, 19(15), 6361–6396. doi:10.1007/s10518-020-01024-6.